AD-A164 697 PHOTOLYSIS OF BRCN BETWEEN 193 AND 266 NM(U) HOWARD UNIV WASHINGTON D C J A RUSSELL ET AL. 30 JAN 86 ONR-TR-21 N00014-80-C-0305 1/1

UNCLASSIFIED F/G 7/4 NL

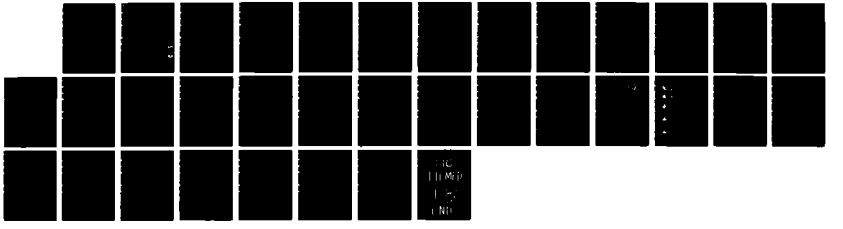

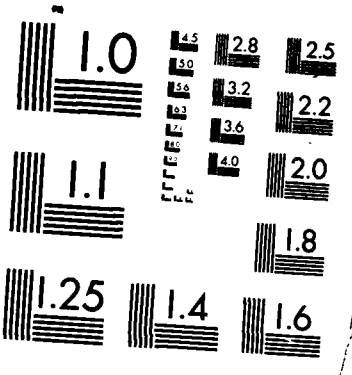

(12)

SECURITY CLASSIFICATION OF THIS PAGE (When Data Entered)

REPORT DOCUMENTATION PAGE		READ INSTRUCTIONS BEFORE COMPLETING FORM
1. REPORT NUMBER ONR-TR- 21	2. GOVT ACCESSION NO.	3. RECIPIENT'S CATALOG NUMBER
4. TITLE (and Subtitle) Photolysis of BrCN between 193 and 266 nm		5. TYPE OF REPORT & PERIOD COVERED TECHNICAL REPORT 6. PERFORMING ORG. REPORT NUMBER
7. AUTHOR(s) J. A. Russell, I. A. McLaren, W. M. Jackson and J. B. Halpern		8. CONTRACT OR GRANT NUMBER(s) N00014-80-C-0305
9. PERFORMING ORGANIZATION NAME AND ADDRESS Laser Chemistry Division Department of Chemistry Howard University, Washington, D.C.		10. PROGRAM ELEMENT, PROJECT, TASK AREA & WORK UNIT NUMBERS NR-051-733
11. CONTROLLING OFFICE NAME AND ADDRESS Office of Naval Research Department of the Navy Arlington, VA 22217		12. REPORT DATE January 30, 1986 13. NUMBER OF PAGES 29
14. MONITORING AGENCY NAME & ADDRESS(if different from Controlling Office)		15. SECURITY CLASS. (of this report) UNCLASSIFIED 15a. DECLASSIFICATION/DOWNGRADING SCHEDULE

16. DISTRIBUTION STATEMENT (of this Report)

Approved for public release; reproduction is permitted for any purpose of the United States Government; distribution is unlimited.

17. DISTRIBUTION STATEMENT (of the abstract entered in Block 20, if different from Report)

Distribution of this document is unlimited.

18. SUPPLEMENTARY NOTES

Prepared for publication in the Journal of Physical Chemistry

19. KEY WORDS (Continue on reverse side if necessary and identify by block number)

Photodissociation, BrCN, Photolysis, UV

20. ABSTRACT (Continue on reverse side if necessary and identify by block number)

Measurement of the quantum state distribution of CN (X) fragments from the photolysis of BrCN at several wavelengths between 193 and 266 nm shows that there is very little excitation of v" greater than 1 levels in the nascent distribution for photlysis below 230 nm. Above this wavelength, significant population is found in excited vibrational states. Scaling of the distributions indicates that the potential energy surface on which the molecules dissociates is simple.

DD FORM 1 JAN 73 1473 EDITION OF 1 NOV 65 IS OBSOLETE S/N 0102-014-6601

UNCLASSIFIED

SECURITY CLASSIFICATION OF THIS PAGE (When Data Entered)

Photolysis of BrCN Between 193 and 266 nm.

Jeffrey A. Russell[#], Ian A. McLaren, William M. Jackson[*] and Joshua B. Halpern[§]

Department of Chemistry

Howard University

Washington, DC 20059

ABSTRACT

Measurement of the quantum state distributions of CN ($X^2\Sigma^+$) fragments from the photolysis of BrCN at several wavelengths between 193 and 266 nm shows that there is very little excitation of $v'' > 1$ levels in the nascent distributions for photolysis below 230 nm. Above this wavelength, significant population is found in excited vibrational states. Scaling of the distributions indicates that the potential energy surface on which the molecules dissociates is simple.

Keywords: Photodissociation

Present address: Avco-Everett Laboratories, Everett, MA

* Present address: Department of Chemistry, University of California at Davis, Davis, California

§ To whom corrspondance is to be addressed

INTRODUCTION

The cyanogen halides have long been a favorite exemplary system for those interested in photodissociation (1-3). The fragmentation patterns are simple, producing halogen atoms and CN radicals. Both of these species are relatively easy to detect. Quantum state distributions of ground state CN radicals can be measured by laser induced fluorescence (LIF) (4) and electronically excited radicals can be characterized by emission spectroscopy (5). Halogen atoms can be monitored by time-of-flight spectroscopy (6), or if they are excited, by their IR emission (7). The earliest work was done on ICN (5-7), whose A continuum has a maximum at 266 nm, the fourth harmonic of the Nd-YAG laser. With the introduction of excimer lasers and non-linear frequency shifting methods, it has become possible to look at the nascent products of the photolysis of BrCN and ClCN as well (8). Several experiments have been done on the photochemistry of BrCN following excitation of its A continuum at different wavelengths (9) and using pulsed seeded beams to cool out any hot band contributions (10, 11).

The original measurement of nascent CN fragment quantum state distributions from the photolysis of BrCN was done at 193 nm by Halpern and Jackson (8). LIF spectra were measured at pressures below a tenth of a millitorr and delays between photolysis and probing of less than 500 ns. Nascent CN quantum state distributions were shown to have less than 6% of the population in $v'' = 1$ and higher vibrational levels. The

rotational distribution in the $v'' = 0$ level is shown in Figure 1a. It is non-thermal, and peaked sharply at about $N = 65$, with a cutoff at about $N = 80$.

It is important to find those conditions under which the distributions are nascent. This is not trivial. Firstly, the CN fragments travel ten times faster than at room temperature. For example, at 193 nm, the slowest CN fragments have over 1.3 eV of translational energy, and the fastest well over 2 eV, even taking into account the possible electronic excitation of the bromine atoms.

In addition, the cross-sections for rotational cooling, and the conversion of translational to vibrational energy by collision of CN fragments, are large. This was clear to us in our original work, where even at pressures of 10^{-2} torr and delays of 0.5 μs one could see changes in the vibrational and rotational distributions.

Recently Hay, Shokoohi, Callister and Wittig have studied the energy transfer mechanism following collisions with foreign gases (12). They showed that levels with $N'' > 70$ were essentially unrelaxed by collisions, while lower rotational levels relax on one or two collisions. Of course, collisional relaxation is more of a problem when the available energy is high than when it is low.

We have been interested in vibrational energy transfer following collisions of the CN fragments with BrCN (13). In this

case the cross-section for collisional relaxation seems to be very large. Especially at the shorter dissociation wavelengths where the amount of energy available to be distributed among the fragment's modes of motion is high, extreme care must be taken to keep the pressure of BrCN low if nascent distributions are to be measured.

This is illustrated by the differences in measured vibrational partitioning in the 193 nm photolysis between the work of Fisher et al. (9), where the percentage of v" = 1 was 16% and that of Halpern and Jackson where it was well under 6% (8). The latter result was confirmed by Hay and co-workers (12). Fisher et al. maintained pressures of BrCN of between 75 and 150 mtorr and used a photolysis-probe delay of 80 - 40 ns for an average $P\tau$ ratio of 8000 mtorr-ns. Halpern and Jackson used pressures of BrCN of less than 0.2 mtorr and delays of about 500 ns. The $P\tau$ ratio in the latter case is 100 mtorr-ns, which is a factor of 80 lower. At room temperature the conditions of Reference 9 would correspond to about 0.08 collisions, but for the fastest CN fragments from the dissociation of BrCN at 193 nm, this would correspond to more than one half of a gas kinetic collision. This accounts for the difference in vibrational partitioning.

Fisher et al. note a decreasing trend in the occupation of vibrationally excited levels of nascent CN fragments, but this is a gradual transition in their work, and is masked by the effects of collision. We present evidence here that the transition is

much sharper, and associated with dissociation along a different potential energy surface of the BrCN.

EXPERIMENTAL

Figure 2 is a sketch of the experimental apparatus. Tunable far UV light was generated by Raman shifting a doubled Nd-YAG pumped dye laser system (Quantel 581C / TDL-50). Light at 193 and 248 nm was generated by a Questek model 2200 excimer laser. The CN ($X^2\Sigma^+$ ---> $B^2\Sigma^+$) LIF spectrum was excited by a Molectron UV-400 nitrogen pumped dye laser. The dye laser output was attenuated so that the LIF signal was not saturated. The two laser beams were counter-propagated through a small vacuum cell. Fluorescence was observed at right angles through a 10 nm bandpass dielectric filter by an EMI 9813 photomultiplier tube.

The experiment was controlled by an IBM-XT computer system using an interface system constructed in our laboratory (14). The LIF signal was captured by a PAR 164 gated integrator that was operated in the linear mode, rather than the exponential mode used in normal boxcar operation. An experimental sequence consisted of firing the dissociating and probe lasers, and gating the PAR 162 integrator. Digitization of the LIF signal on every shot, together with active baseline correction and measurement of the dye laser output energy, permitted accurate signal normalization on a shot-to-shot basis. Photolysis laser intensities were observed to remain constant over the course of each run and were not corrected for. After a set number of pulses a stepping motor attached to the dye laser sine drive was advanced.

BrCN was obtained from Fisher Scientific. It was placed in a cold finger and pumped on for a few minutes before being used.

RESULTS

Figure 1 shows the LIF spectra for photolysis at 193, 200, 220, 240, and 248 nm. Spectra characteristic of 266 nm can be found in Reference 12. At 193 and 248 nm, the pressure of BrCN was less than 1 mtorr. Otherwise the BrCN pressure was between 10 and 40 mtorr. The time between the photolysis and probe lasers was 80 ns, with a maximum jitter of less than 10 ns. We have also measured spectra following photolysis of BrCN at 230 nm, and at several wavelengths between 242 and 240 nm.

The spectra show that the CN is always formed rotationally hot, but that there is significant vibrational excitation only above 240 nm. The shapes of the distributions are also seen to broaden in the 240 nm region.

To characterize these data, we plotted the most probable and highest observed rotational state in each spectrum versus the total available energy following photolysis in Figure 3. In addition we included the results of Wittig's group at 266 nm (11). Above 240 nm, the results fall on separate straight lines for the mode and maximum of the distributions. Below 240 nm, the results also fall on two lines but are displaced from the first set. We can force all of the points to fall on the same line by assuming that the photolysis above 240 nm results only in the formation of Br ($^2P_{3/2}$) and that below only Br ($^2P_{1/2}$) is formed. Below 240 nm the amount of available energy would decrease by 3668 cm^{-1}.

There are no published far-UV absorption spectra of BrCN. King and Richardson display only a schematic representation of the spectrum (15). Figure 4 shows the absorption spectrum of BrCN measured in a Beckman DU-5 spectrophotometer. BrCN was placed in a 1 cm cell and allowed to equilibrate. The gas pressure was taken as the vapor pressure of BrCN (16).

DISCUSSION

The heats of formation of BrCN, CN ($X^2\Sigma^+$) and Br ($^2P_{3/2}$) are 46.1 ± 1.5, 101 ± 1 and 28.18 ± 0.02 kcal/mol respectively (3). Thus the thermochemical limit for dissociation is 29,050 ± 900 cm^{-1} or 344 ± 10 nm. The Br atoms can also be produced in the $^2P_{1/2}$ state, which lies 3678 cm^{-1} above the ground state. The first three columns of Table I list photolysis wavelengths, and the amount of available energy associated with each of the low-lying Br atom states.

Two recurring themes in research on the photolysis of cyanogen halides have been the determination of quantum yields of the $^2P_{1/2}$ and $^2P_{3/2}$ states, and the parsing of CN fragment quantum state distributions to separate the components associated with each ^2P state. We will attempt to treat both of these matters by consideration of the measured CN fragment distributions.

Most of the spectra in Figure 1 have similar shapes. We sought a scaling that would emphasize this. The best results were obtained by plotting the rotational state distributions as functions of the ratio of rotational energy to total available energy, where the latter has been chosen on the criterion of best fit. We were guided in this choice by our interpretation of Figure 3. The fourth column of Table I lists the choice that was made for the available energy at each wavelength. Figure 5

shows the rotational distributions obtained after correction for LIF probe laser intensity and rotational line strengths.

This figure lends credence to our assumption that only $^2P_{1/2}$ bromine atoms are produced at wavelengths below 240 nm. At 240 nm and above, the primary product dissociation channel seems to produce $^2P_{3/2}$ bromine atoms. Examination of Figure 5 shows that there is a second hump on the CN state distributions at 248 and 242 nm, which corresponds to the production of the $^2P_{1/2}$ state. If one subtracts the scaled distribution at 193 nm, from those at 242 and 248 nm, and then shifts the remainder to account for the 3468 cm^{-1} of electronic energy in excited bromine, one is left with a second, overlaying rotational distribution corresponding to the production of CN radicals and Br ($^2P_{1/2}$) atoms. In addition, if one assumes that v" = 1 CN radicals produced at 248 and 242 nm are associated with the production of Br ($^2P_{3/2}$), then the rotational distribution of the v" = 1 CN matches closely, though not exactly those shown in Figure 5.

As was shown in Reference 8, such rotational distributions are closely associated with the distribution of impact parameters. Given the available energy, E_{avl}, and the rotational energy, E_R,

$$b = [(m_{CN}/m_{Br-CN})(1-E_R/E_{AVL})]^{1/2} r_e \quad (1)$$

where m_x is the mass of x and r_e the separation between the Br and CN. If the distribution of CN products as a function of the ratio E_r/E_{avl} is the same for all of the measured wavelengths,

the distribution of impact parameters must also be the same. This implies that the Br and CN fragments are separating on the same surface at all wavelengths. The fragments are spinning apart with the same relative distance and orientation between the bromine atom and the CN fragment. In other words the potential energy surface upon which the dissociation takes place is the same over this entire range of photolysis wavelengths, at least as far as the angular motion is concerned.

Rotational distributions from the photolysis of ClCN and BrCN are peaked at high rotational states corresponding to about 40 % of the available energy appearing in rotation. Photolysis of ICN leaves most of the CN products in relatively low rotational levels. Waite, Heljavian, Dunlap and Baronavski evaluated potential energy surfaces to explain the observed rotational distributions in the photolysis of cyanogen halides (17). They found that the observed distributions from photolysis of ICN required a surface such as that shown in Figure 6a, while the type of surface shown in Figure 6b resulted in distributions typical of the photolysis of BrCN and ClCN. We suggested a similar potential for the photolysis of BrCN and ClCN in Reference 10, with the addition of a shallow valley.

When a dissociating molecule moves on the potential energy surface of Figure 6a the initial motion results in a rapid bending, which can be converted to rotation of the diatomic fragment. However this motion is slowed as the fragment encounters the second hill of the potential. This deceleration

can also convert the motion into vibrational excitation of the diatomic fragment. The motion of the CN fragment on the simpler surface of Figure 6b, is just a rapid conversion of the bending motion into rotational excitation of the diatomic radical and orbital angular momentum of the separating fragments.

Waite et al. showed by calculation that the results were not much affected if one started with a 0 or 300 K distribution of parent molecules. This is in agreement with the results of Reference 11 on BrCN photolysis at 193 nm and those of Reference 17 on the photolysis of ICN at 266 nm. However, it is in disagreement with the results of Reference 11 on the photolysis of BrCN at 266 nm. In the latter case, it was found that photolysis of the cold BrCN produced only a small amount of CN in a few low rotational states, while photolysis of the BrCN at room temperature resulted in a much stronger signal with a distribution similar to that observed in this work. Consideration of these results and Figure 4 shows that the absorption at 266 nm is vanishingly small, and probably dominated by absorption to the hot bands. As one moves further to the UV, the role of hot bands in the absorption should decrease drastically.

One is then left to consider the mechanism for production of the different electronic states of bromine, and vibrationally excited CN radicals. Figure 7a shows a simple, one-dimensional surface. For such a potential, the absorption spectrum can be obtained by the reflection principal as was done in Wilson's

pioneering work on the photolysis of ICN. The shift from the channel producing $^2P_{1/2}$ and $^2P_{3/2}$ Bromine is controlled by the Franck-Condon principal.

The strength of the CN bond is several times that of the Br-C bond. Rather than viewing the vibration of BrCN in terms of a normal mode picture, one may consider a local mode structure, with the CN vibrational excitation isolated in the triatomic molecule. Thus, the surface leading to v" = 1 CN and $^2P_{3/2}$ Br lies parallel to and about 2000 cm^{-1} above the lowest dissociation curve. If there is no production of $^2P_{3/2}$ Br below 240 nm, then we can assume that none of the curves leading to different electronic states cross, although they may not be exactly parallel at all times. The curves producing different vibrational levels of the CN fragment and the same electronic state of the bromine atom are parallel to the extent that the local mode picture obtains. Since the vibrational frequency of CN is 2064 cm^{-1} and that of the ν_1 mode of BrCN is 2000 cm^{-1}, they are probably reasonably parallel.

Figure 7a seems to imply that at some intermediate wavelength one should produce more v" = 1 CN product than v" = 0. However, it does not take account of the Franck-Condon factors involving the CN group in the BrCN molecule. All of the ground state BrCN will have zero quanta in the CN stretch mode. In comparison to CN electronic spectra, the Franck-Condon factor for absorption to states where the CN is unexcited should be several times greater than excitation to states where the CN stretch is

For potentials like Figure 6a, where the fragments can chatter against each other, a great deal of vibrational excitation could be produced. Similarly, vibrational excitation can be produced in linear-to-linear excitations leading to dissociative states, as the separating fragments can interact to activate vibrational modes of the fragments.

Figure 7b shows an alternative model of the electronic state potential energy surface. In this case the states leading to Br ($^2P_{1/2}$) and Br ($^2P_{3/2}$) cross, with the latter rising sharply. At low energies only the lower curve leading to $^2P_{3/2}$ atoms can be reached. At slightly higher energies one can excite both the lower curve to the left of the crossing point and the upper curve to the right of the crossing. This will produce a mixture of both Br atom states. Finally at high photon energies only the upper electronic state can be populated, which leads to $^2P_{1/2}$ bromine atoms.

CONCLUSIONS

It has been shown that the nascent quantum state distributions of CN fragments from the photolysis of BrCN between 193 and 248 nm can be scaled to each other. This scaling implies a limit at about 235 nm for the production of Br ($^2P_{3/2}$), and that the dissociative potential energy surface has a particularly simple form.

ACKNOWLEDGEMENT

This work was supported by the Office of Naval Research. Jeffrey A. Russell was supported by NASA under grant number NAGW-446. Ian A. McLaren acknowledges the support of the SOHIO Corporation. Joshua Halpern was partially supported by NSF grant CHE8219255.

REFERENCES

1. H. Okabe, The Photochemistry of Small Molecules, Wiley Interscience, New York, 1978.

2. M. N. R. Ashfold, M. T. MacPherson and J. P. Simmons, Topics in Current Chemistry, Volume 86, Springer Verlag, Berlin (1979). p. 1.

3. H. Okabe and W. M. Jackson, to appear in Annual Reviews of Physical Chemistry, 1985. D. Volman editor.

4. W. M. Jackson and R. J. Cody, J. Chem. Phys., 61 (1974) 4183.

5. M. N. R. Ashfold and J. P. Simons, J. Chem. Soc. Faraday Trans. II, 73 (1977) 858; 74 (1978) 280.

6. J. H. Ling and K. R. Wilson, J. Chem. Phys., 63 (1975) 101.

7. W. M. Pitts and A. P. Banonavski, Chem. Phys. Lett., 71 (1980) 395.

8. J. B. Halpern and W. M. Jackson, J. Phys. Chem., 86 (1982) 3528.

9. W. H. Fisher, R. Eng, T. Carrington, C. H. Dugan, S. V. Filseth and C. M. Sadowski, J. Chem. Phys., 89 (1984) 457.

10. R. Lu, V. McCrary, J. B. Halpern, J. Phys. Chem., 88 (1984) 3419.

11. I. Nadler, H. Reisler and C. Wittig, Chem. Phys. Lett., 103 (1984) 451.

12. S. Hay, F. Shokoohi, S. Callister and C. Wittig, Chem. Phys. Lett., 118 (1985) 6.

13. In preparation

14. I. A. McLaren, private communication

15. G. W. King and A. W. Richardson, J. Mol. Spectrosc., 21 (1966) 339.

16. Handbook of Chemistry and Physics, 62nd Edition, Chemical Rubber Company Press, Boca Raton, Florida, 1981, p. D-174.

17. B. Waite, H. Helvajian, B. J. Dunlap and A. P. Baronavski, Chem. Phys. Lett., 111 (1984) 544.

TABLE I

Laser Wavelength nm	(Frequency) cm^{-1}	Excess Energy in cm^{-1} $Br(^2P_{3/2})$	$Br(^2P_{1/2})$	Major Channel	Highest J	(Mean) $E_{Rotational}$
193	51,813	22,763	19,095	$^2P_{1/2}$	84(62)	13,566 (7,421)
202	49,505	20,455	16,787	$^2P_{1/2}$	77(56)	11,411 (6,065)
220	45,454	16,404	12,736	$^2P_{1/2}$	68(51)	8,915 (5,039)
242	41,322	12,272	8,604	$^2P_{3/2}$	66(52)	8,402 (5,236)
248	40,322	11,272	7,604	$^2P_{3/2}$	62(49)	7,421 (4,655)

FIGURE CAPTIONS

Figure 1: Sketch of the experimental apparatus. Photolysis light was generated either with an excimer laser using KrF (248 nm) or ArF (193 nm), or doubled and anti-Stokes Raman shifted light from a Nd-YAG pumped dye laser. This UV light is sent into a small cell co-axially with light from a Nitrogen laser pumped dye laser which excited the LIF spectra of nascent CN fragments. The lasers were fired by a computer controlled data acquisition system which also monitored the LIF signal, and the intensities of the two lasers.

Figure 2: Experimentally observed LIF spectra of nascent CN radical fragments following the photolysis of BrCN at several wavelengths. The R branch is shown only for the 248 nm spectrum.

Figure 3: Rotational states of maximum probability and the last observed state as functions of the total available energy taken from Figure 2. The point for 266 nm is taken from Reference 11. The bars represent estimates of error from the data. The dots refer to the peaks of the observed distribution and the crosses to the highest observed rotational states in the v" = 0 level. There is a discontinuity at about 230 nm. As discussed in the text, the points above 230 nm can be associated with the production of $Br(^2P_{3/2})$ and those below 230 nm with the production of $Br(^2P_{1/2})$.

Figure 4: Absorption spectrum of BrCN at room temperature in a 1 cm cell as measured by a DU-4 spectrophotometer.

Figure 5: Scaled rotational distributions from Figure 2. The scaling method is described in the discussion. Briefly this involved decreasing the avaliable energy by the electronic energy of Br($^2P_{1/2}$) where suggested by the results of Figure 3.

Figure 6: Potential energy surfaces suggested by Waite, et al (17) for the photolysis of ICN (6a) and ClCN (6b). The coordinate system is taken so the CN moity is oriented as shown in the diagrams. The potential energy surface on which the BrCN separates must be much like that in Figure 6b.

Figure 7: Electronic potential energy surfaces for the production of Br $^2P_{3/2}$ and $^2P_{1/2}$ and v" = 1 CN fragments. See the text for a more complete discussion.

Figure 1

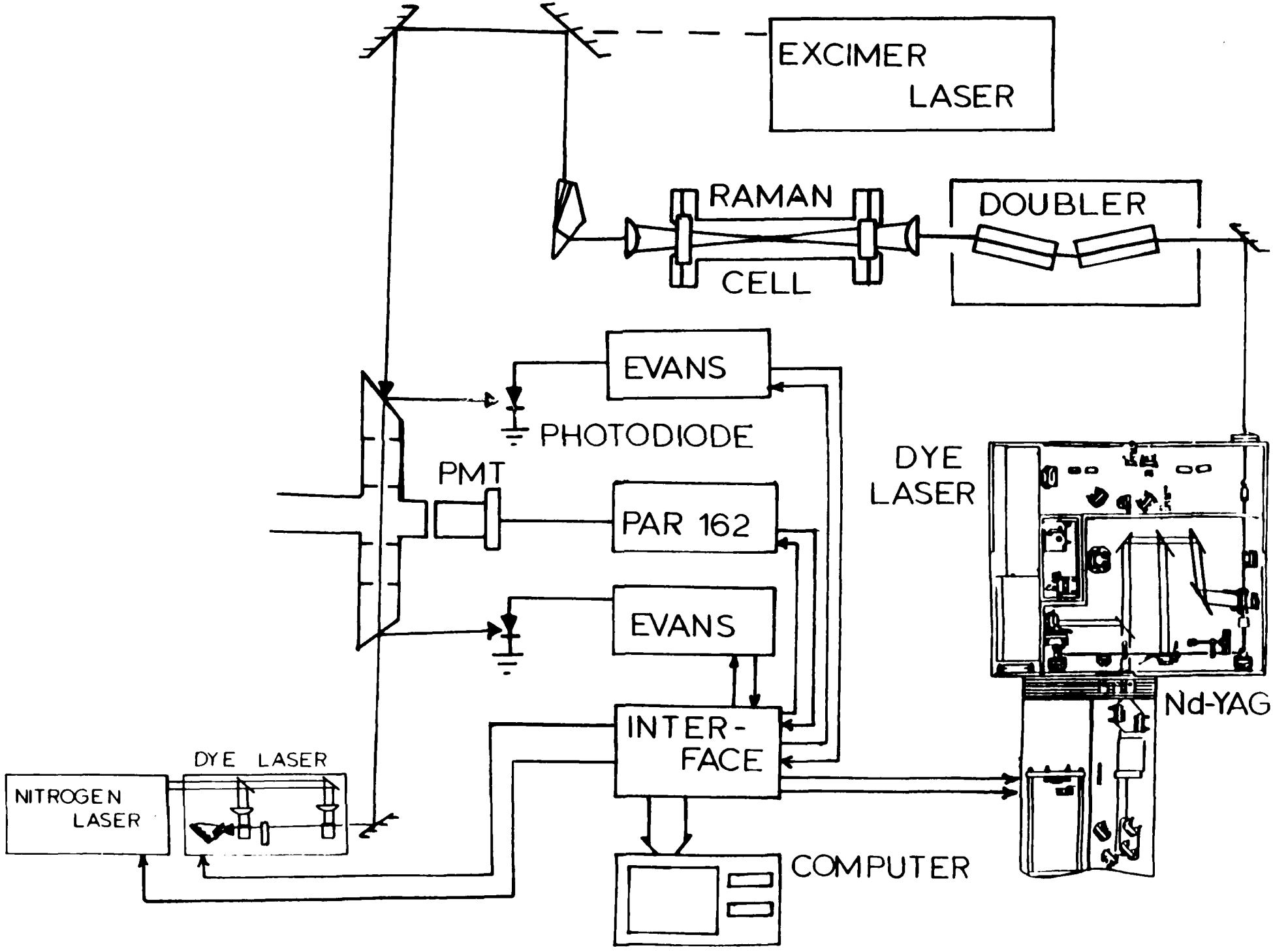
EXCIMER
LASER
RAMAN
CELL
DOUBLER
EVANS
PHOTODIODE
PMT
PAR 162
EVANS
DYE
LASER
Nd-YAG
INTER-
FACE
DYE LASER
NITROGEN
LASER
COMPUTER

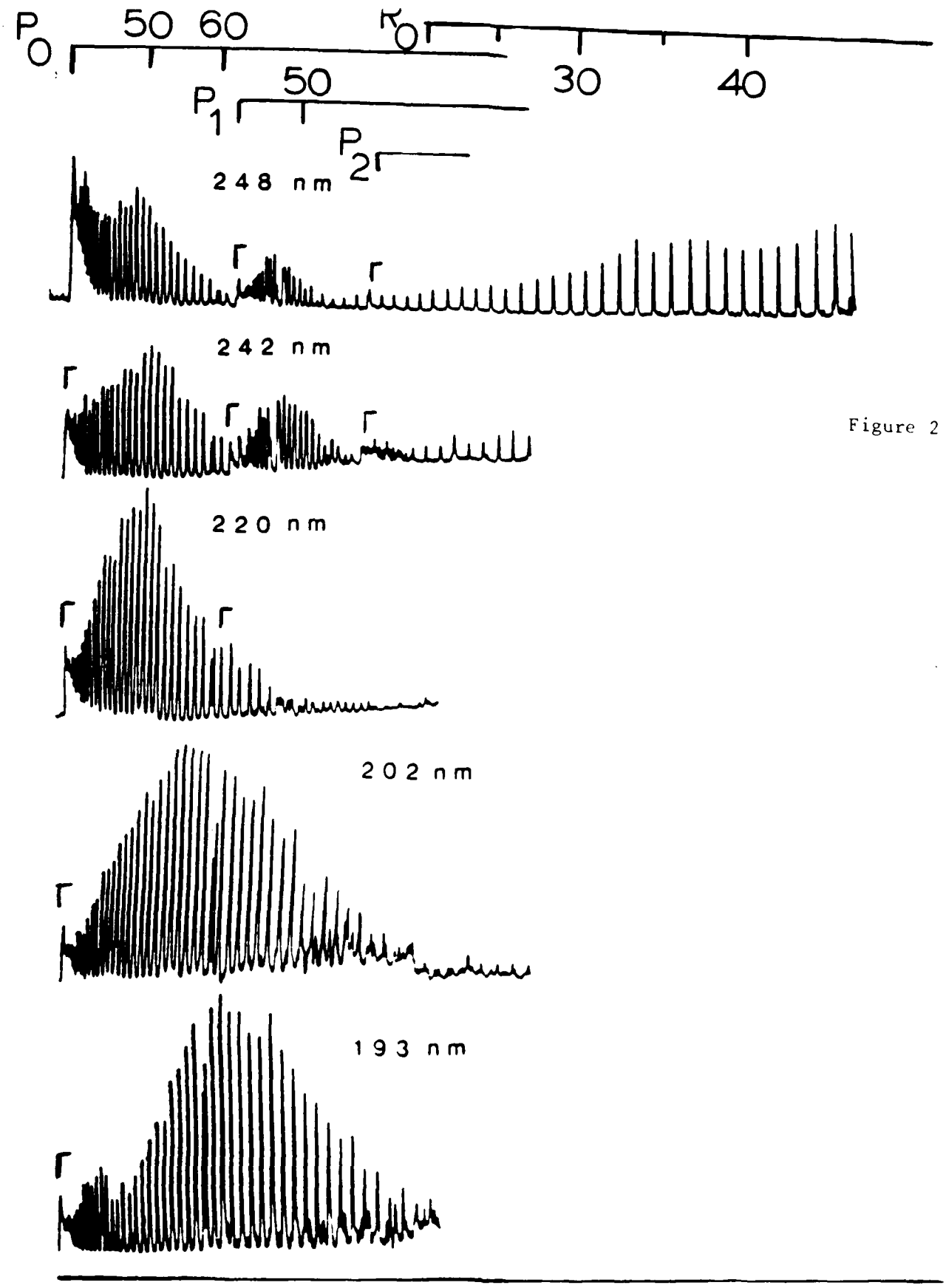
P0
50 60
R0
30
40
P1
50
P2
248 nm
242 nm
220 nm
202 nm
193 nm
WAVELENGTH nm

Figure 2

Figure 3

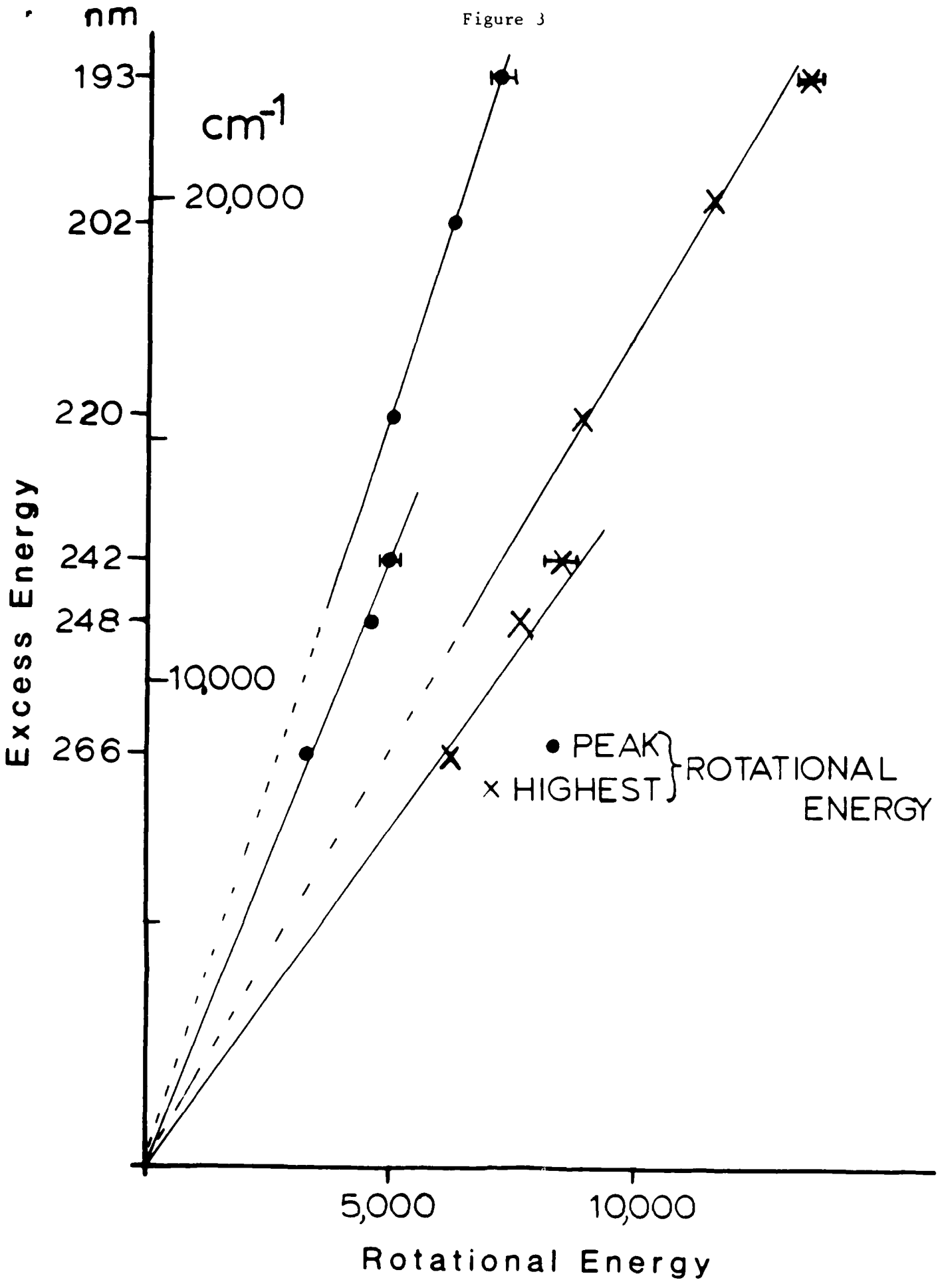
nm
193
cm-1
20,000
202
220
242
248
10,000
266
Excess Energy
• PEAK
× HIGHEST
ROTATIONAL ENERGY
5,000
10,000
Rotational Energy

Figure 4

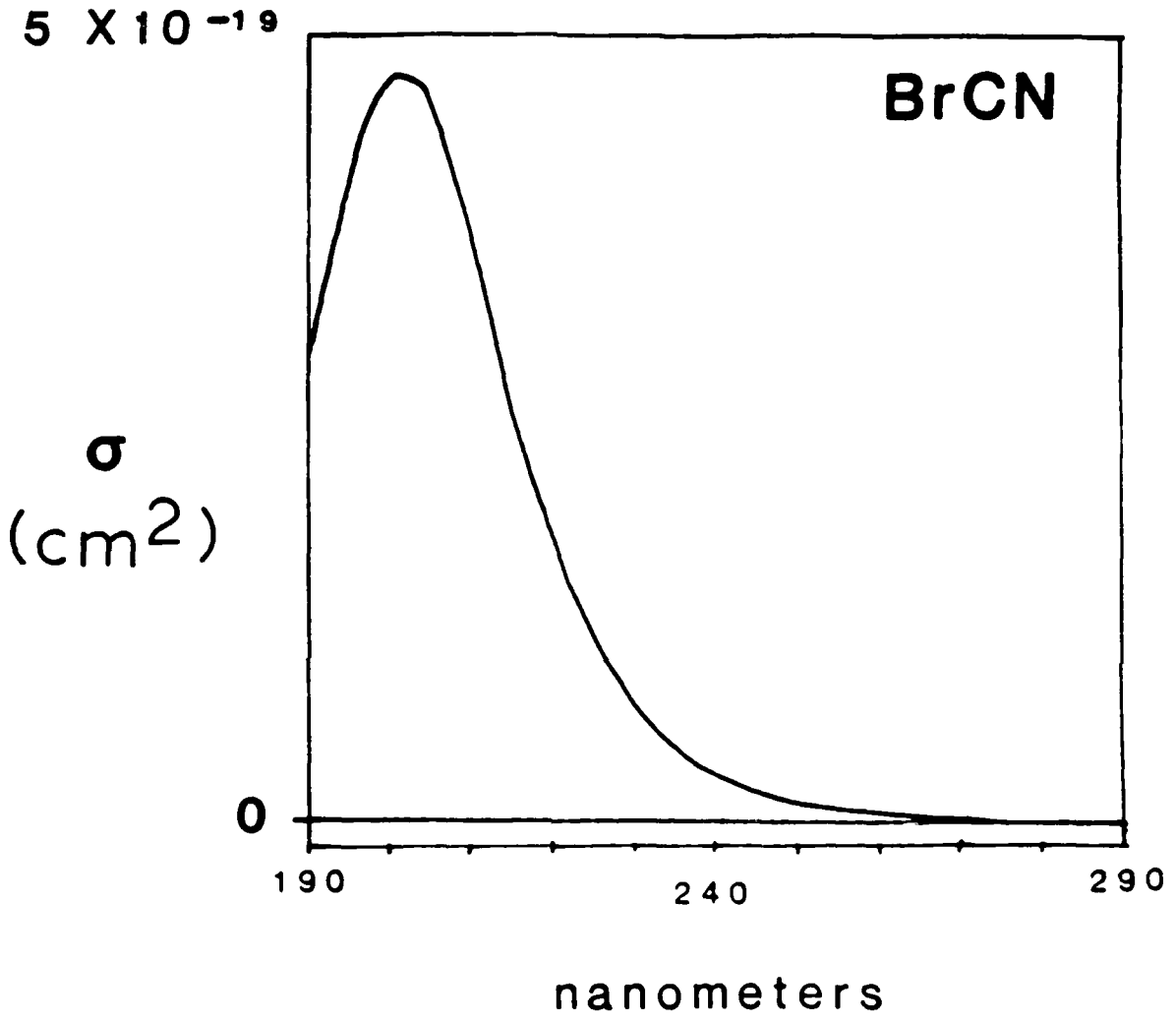

Figure 5

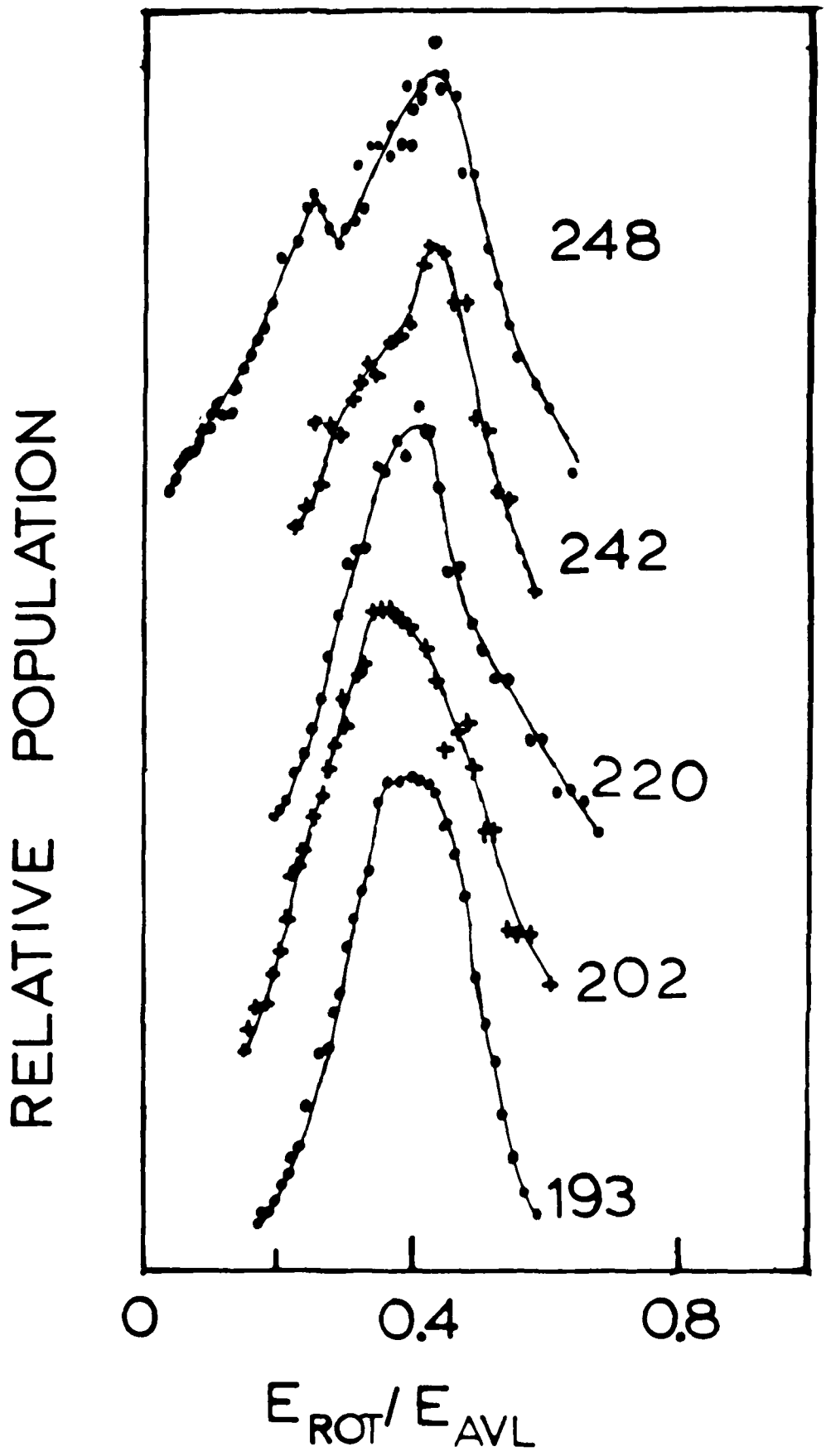

Figure 6a

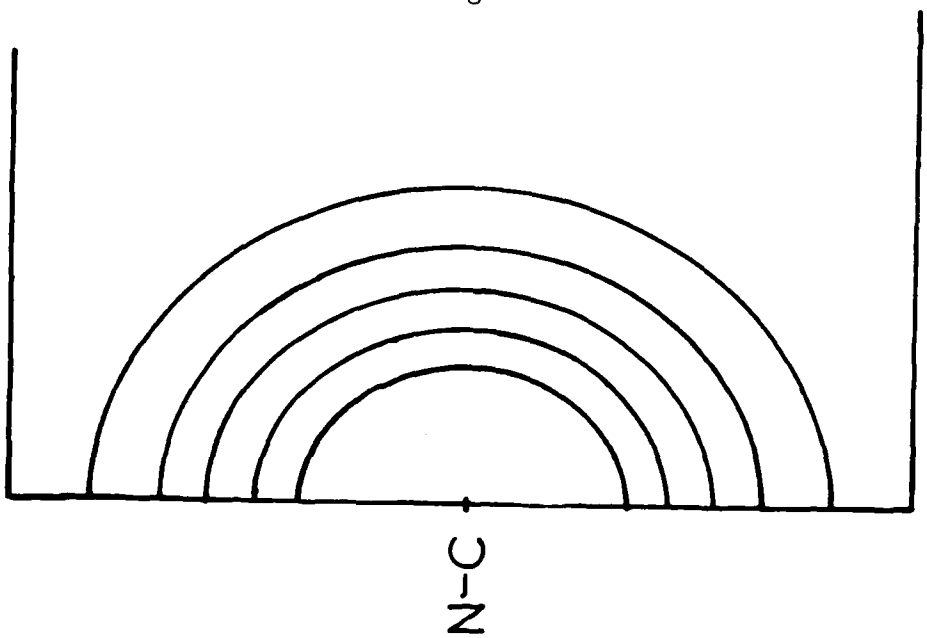

Figure 6b

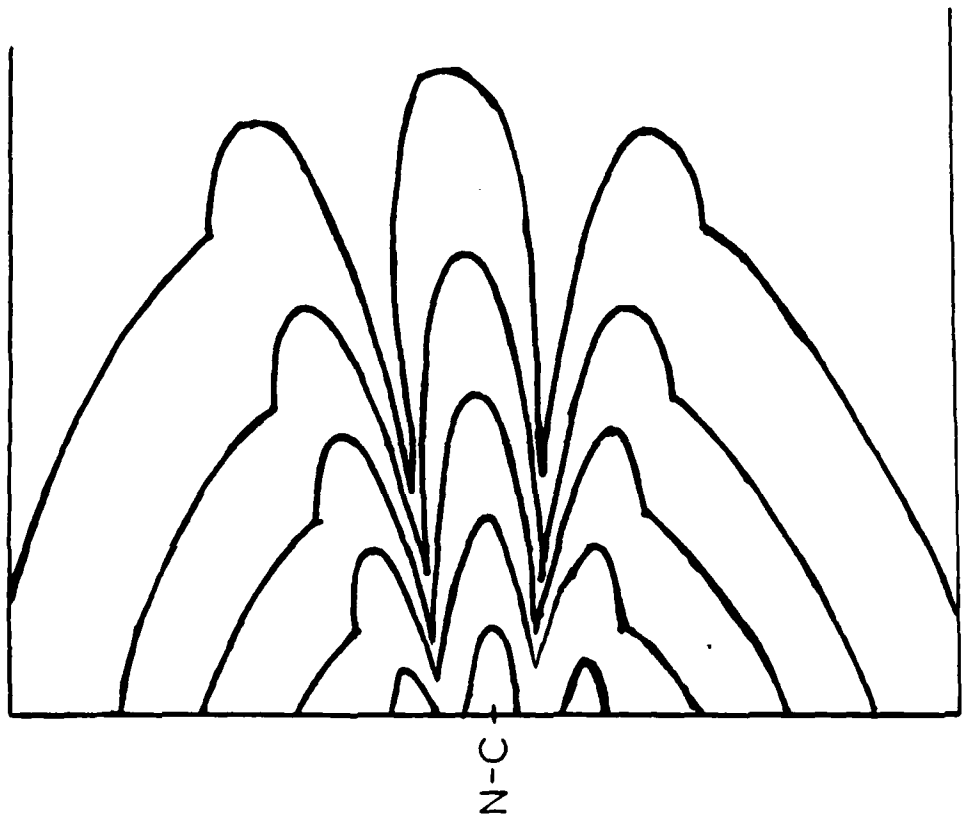

Figure 7a

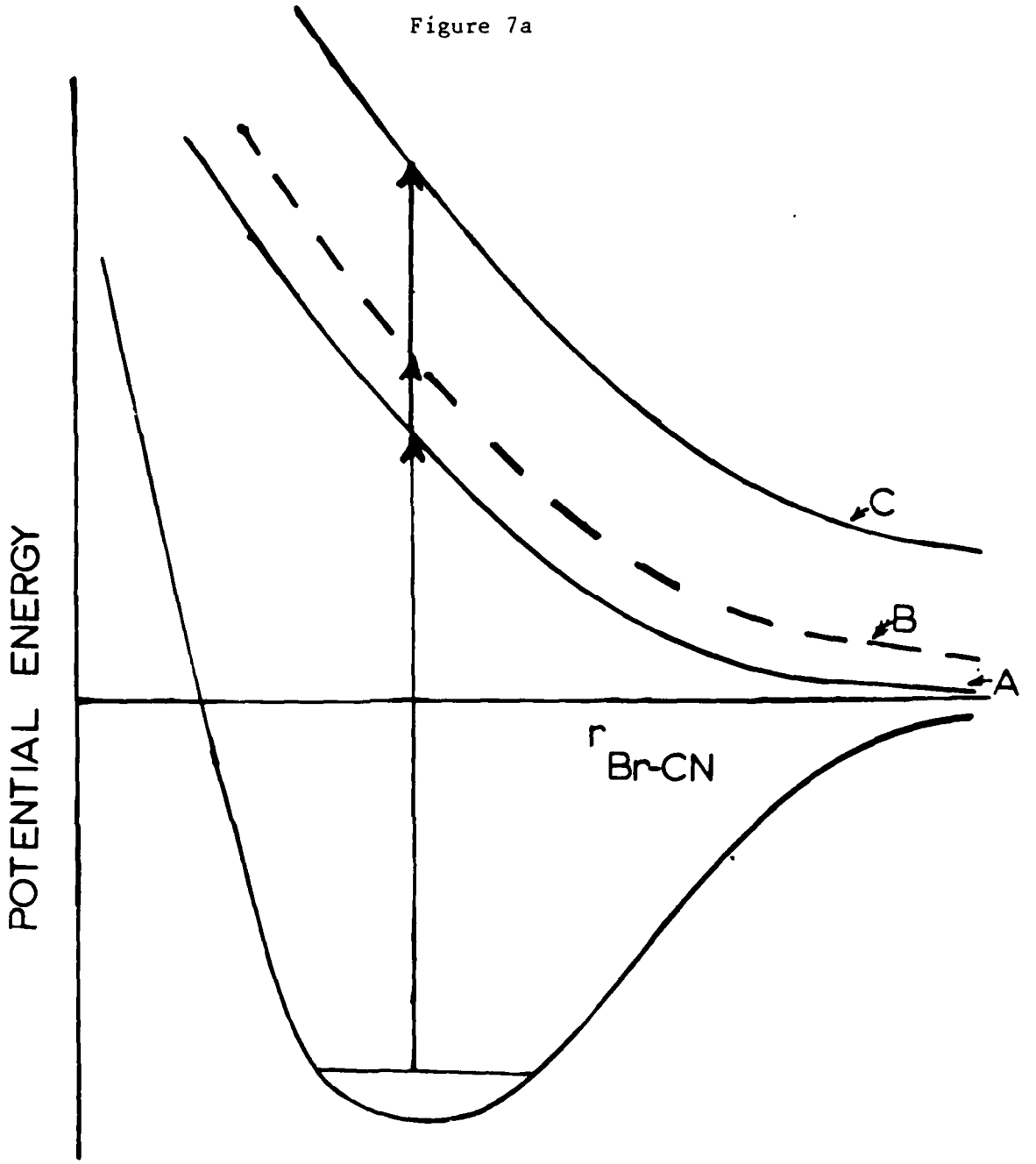

Figure 7b

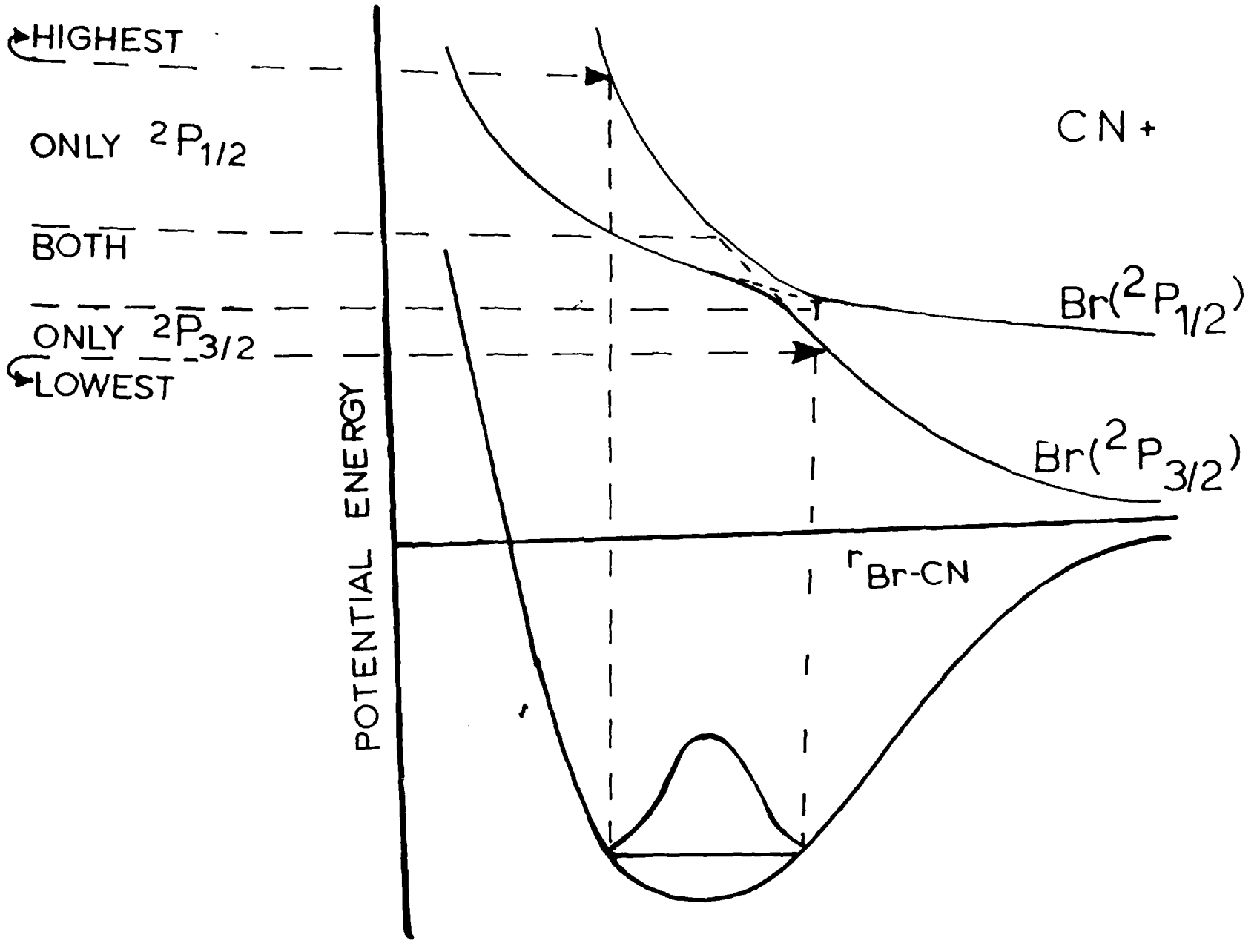
HIGHEST
ONLY $^2P_{1/2}$
BOTH
ONLY $^2P_{3/2}$
LOWEST
POTENTIAL ENERGY
CN +
Br($^2P_{1/2}$)
Br($^2P_{3/2}$)
r_{Br-CN}

DL/413/83/01
GEN/413-2

TECHNICAL REPORT DISTRIBUTION LIST, GEN

	No. Copies
Office of Naval Research Attn: Code 413 800 N. Quincy Street Arlington, Virginia 22217	2
Dr. Bernard Douda Naval Weapons Support Center Code 5042 Crane, Indiana 47522	1
Commander, Naval Air Systems Command Attn: Code 310C (H. Rosenwasser) Washington, D.C. 20360	1
Naval Civil Engineering Laboratory Attn: Dr. R. W. Drisko Port Hueneme, California 93401	1
Defense Technical Information Center Building 5, Cameron Station Alexandria, Virginia 22314	12
DTNSRDC Attn: Dr. G. Bosmajian Applied Chemistry Division Annapolis, Maryland 21401	1
Dr. William Tolles Superintendent Chemistry Division, Code 6100 Naval Research Laboratory Washington, D.C. 20375	1
Dr. David Young Code 334 NORDA NSTL, Mississippi 39529	1
Naval Weapons Center Attn: Dr. Ron Atkins Chemistry Division China Lake, California 93555	1
Scientific Advisor Commandant of the Marine Corps Code RD-1 Washington, D.C. 20380	1
U.S. Army Research Office Attn: CRD-AA-IP P.O. Box 12211 Research Triangle Park, NC 27709	1
Mr. John Boyle Materials Branch Naval Ship Engineering Center Philadelphia, Pennsylvania 19112	1
Naval Ocean Systems Center Attn: Dr. S. Yamamoto Marine Sciences Division San Diego, California 91232	1

OL/413/83/01
051A/413-2

TECHNICAL REPORT DISTRIBUTION LIST, 051A

Dr. M. A. El-Sayed
Department of Chemistry
University of California
Los Angeles, California 90024

Dr. E. R. Bernstein
Department of Chemistry
Colorado State University
Fort Collins, Colorado 80521

Dr. J. R. MacDonald
Chemistry Division
Naval Research Laboratory
Code 6110
Washington, D.C. 20375

Dr. G. B. Schuster
Chemistry Department
University of Illinois
Urbana, Illinois 61801

Dr. J.B. Halpern
Department of Chemistry
Howard University
Washington, D.C. 20059

Dr. M. S. Wrighton
Department of Chemistry
Massachusetts Institute of Technology
Cambridge, Massachusetts 02139

Dr. A. Paul Schaap
Department of Chemistry
Wayne State University
Detroit, Michigan 49207

Dr. W.E. Moerner
I.B.M. Corporation
5600 Cottle Road
San Jose, California 95193

Dr. A.B.P. Lever
Department of Chemistry
York University
Downsview, Ontario
CANADA M3J1P3

Dr. John Cooper
Code 6173
Naval Research Laboratory
Washington, D.C. 20375

Dr. George E. Walrafen
Department of Chemistry
Howard University
Washington, D.C. 20059

Dr. Joe Brandelik
AFWAL/AADO-1
Wright Patterson AFB
Fairborn, Ohio 45433

Dr. Carmen Ortiz
Consejo Superior de
Investigaciones Cientificas
Serrano 121
Madrid 6, SPAIN

Dr. John J. Wright
Physics Department
University of New Hampshire
Durham, New Hampshire 03824

Dr. Kent R. Wilson
Chemistry Department
University of California
La Jolla, California 92093

Dr. G. A. Crosby
Chemistry Department
Washington State University
Pullman, Washington 99164

Dr. Theodore Pavlopoulos
NOSC
Code 521
San Diego, California 91232

DTIC

FILMED

4-86

END